



A Dual Interaction Between the 5'- and 3'-Ends of the Melon Necrotic Spot Virus (MNSV) RNA Genome Is Required for Efficient Cap-Independent Translation

Manuel Miras¹, Ana M. Rodríguez-Hernández^{1,2}, Cristina Romero-López³, Alfredo Berzal-Herranz³, Jaime Colchero⁴, Miguel A. Aranda¹ and Verónica Truniger^{1*}

¹ Centro de Edafología y Biología Aplicada del Segura, Consejo Superior de Investigaciones Científicas (CEBAS-CSIC), Murcia, Spain, ² Centro de Investigación en Química Aplicada, Consejo Nacional de Ciencia y Tecnología (CONACYT), Saltillo, Mexico, ³ Instituto de Parasitología y Biomedicina López-Neyra, Consejo Superior de Investigaciones Científicas (IPBLN-CSIC), Granada, Spain, ⁴ Departamento de Física, Edificio CIOyN, Universidad de Murcia, Campus de Espinardo, Murcia, Spain

OPEN ACCESS

Edited by:

Ricardo Flores,
Instituto de Biología Molecular y
Celular de Plantas (IBMCP), Spain

Reviewed by:

K. Andrew White,
York University, Canada
Aurelie Rakotondrifara,
University of Wisconsin–Madison,
United States

*Correspondence:

Verónica Truniger
truniger@cebas.csic.es

Specialty section:

This article was submitted to
Virology,
a section of the journal
Frontiers in Plant Science

Received: 09 March 2018

Accepted: 20 April 2018

Published: 09 May 2018

Citation:

Miras M, Rodríguez-Hernández AM, Romero-López C, Berzal-Herranz A, Colchero J, Aranda MA and Truniger V (2018) A Dual Interaction Between the 5'- and 3'-Ends of the Melon Necrotic Spot Virus (MNSV) RNA Genome Is Required for Efficient Cap-Independent Translation. *Front. Plant Sci.* 9:625. doi: 10.3389/fpls.2018.00625

In eukaryotes, the formation of a 5'-cap and 3'-poly(A) dependent protein–protein bridge is required for translation of its mRNAs. In contrast, several plant virus RNA genomes lack both of these mRNA features, but instead have a 3'-CITE (for cap-independent translation enhancer), a RNA element present in their 3'-untranslated region that recruits translation initiation factors and is able to control its cap-independent translation. For several 3'-CITEs, direct RNA-RNA long-distance interactions based on sequence complementarity between the 5'- and 3'-ends are required for efficient translation, as they bring the translation initiation factors bound to the 3'-CITE to the 5'-end. For the carmovirus melon necrotic spot virus (MNSV), a 3'-CITE has been identified, and the presence of its 5'-end *in cis* has been shown to be required for its activity. Here, we analyze the secondary structure of the 5'-end of the MNSV RNA genome and identify two highly conserved nucleotide sequence stretches that are complementary to the apical loop of its 3'-CITE. In *in vivo* cap-independent translation assays with mutant constructs, by disrupting and restoring sequence complementarity, we show that the interaction between the 3'-CITE and at least one complementary sequence in the 5'-end is essential for virus RNA translation, although efficient virus translation and multiplication requires both connections. The complementary sequence stretches are invariant in all MNSV isolates, suggesting that the dual 5'–3' RNA:RNA interactions are required for optimal MNSV cap-independent translation and multiplication.

Keywords: 3'-CITE, cap-independent translation, MNSV, RNA structure, plant virus, RNA:RNA interactions, translation initiation, translational enhancer

INTRODUCTION

Viral mRNAs have evolved numerous mechanisms for recruiting the host's translational machinery, allowing them to compete with host mRNAs and avoid defense mechanisms that act at the level of translation. Thus, while most plant-encoded mRNAs contain a 5'-cap and a 3'-poly(A) tail that act synergistically to stimulate translation, ~80% of known positive-strand RNA plant

viruses lack one or both of these features in their genomic and subgenomic RNAs (van Regenmortel et al., 2000; Miras et al., 2017a), and they often use their 5'- and/or 3'-termini in alternative gene expression strategies (Nicholson and White, 2011; Truniger et al., 2017). Cap-independent translation in some plant virus RNAs is facilitated by highly structured RNA elements residing within the 5'-untranslated region (5'-UTR), in some cases corresponding to internal ribosomal entry sites (IRES) (Kneller et al., 2006; Zhang et al., 2015; Miras et al., 2017a). In other plant viruses that lack both the cap and 3'-poly(A) tail, such as members of the family *Tombusviridae* and the genus *Luteovirus* (family *Luteoviridae*), RNA elements capable of controlling cap-independent translation residing within their 3'-UTR (abbreviated 3'-CITE for cap-independent translation enhancer) are required for viral RNA translation. Often, *cis*-acting signals residing in the 5'-UTR are also needed for cap-independent translation (Miller and White, 2006; Simon and Miller, 2013; Truniger et al., 2017).

3'-CITEs vary in sequence and folding structure. Based on their RNA structure, seven different types have been identified to date, all in viruses belonging to the family *Tombusviridae*: BTE-like (cloverleaf shape), TED-like (long stem-loop), PTE-like (stem ending with two short connected helical branches), Y-shaped (YSS), I-shaped (ISS), T-shaped (TSS), and CXTE-like 3'-CITEs (Nicholson and White, 2011; Simon and Miller, 2013; Truniger et al., 2017). The last 3'-CITE in this list, CXTE, was identified in two isolates of the carmovirus melon necrotic spot virus (MNSV), MNSV-N and -GX, and was very likely acquired from cucurbit aphid-borne yellows virus (CABYV) through separate interfamilial recombination events (Miras et al., 2014; Truniger et al., 2017). These results show that, in nature, 3'-CITEs are modular and transferable RNA elements. The transfer of 3'-CITEs among viruses confers them with adaptive advantages. 3'-CITEs bind host translation initiation factor eIF4E, as shown for the TED-like (Gazo et al., 2004), YSS (Nicholson et al., 2013), ISS (Nicholson et al., 2010; Miras et al., 2017b), PTE-like (Batten et al., 2006; Wang et al., 2009, 2011) and BTE-like (Treder et al., 2008; Kraft et al., 2013) 3'-CITEs. These results and the observation that several 3'-CITEs continued facilitating cap-independent translation *in vitro* when moved to the 5'-terminus of viral RNAs, thereby replacing their endogenous 5'-UTR (Meulewaeter et al., 1998b; Guo et al., 2000), suggest that the 3'-CITE must be responsible for recruiting the host factors involved in translation initiation and that these must be delivered to the 5'-end near the start codon. Thus, often the presence of both genome ends has been shown to be essential for cap-independent translation (Truniger et al., 2017).

For several types of 3'-CITEs this delivery has been shown or proposed to occur through an interaction based on sequence complementarity between the 3'-CITE and the 5'-end (Simon and Miller, 2013; Truniger et al., 2017). Experimentally, this has been shown for the BTE of barley yellow dwarf virus (BYDV) (Guo et al., 2001), the PTE of saguaro cactus virus (SCV) (Chattopadhyay et al., 2011), the TED of pelargonium line pattern virus (PLPV) (Blanco-Pérez et al., 2016), the YSS of carnation italian ringspot virus (CIRV) (Nicholson and White, 2008; Nicholson et al., 2013) and of tomato bushy

stunt virus (TBSV) (Fabian and White, 2004, 2006), and for the ISS of maize necrotic streak virus (MNeSV) (Nicholson et al., 2010). On the other hand, proposed 5'-3' interactions could not be experimentally confirmed for several viruses, for example, satellite tobacco necrosis virus (STNV) or Red clover necrotic mosaic virus (RCNMV) (Meulewaeter et al., 1998a; Sarawaneeyaruk et al., 2009). Additionally, for tobacco necrosis virus isolate TNV-D, a recent publication shows that the base-pairing between its 5'-UTR and its BTE is not required *in vivo* for efficient virus multiplication (Chkuaseli et al., 2015). 5'-3' interaction can also occur indirectly through ribosomes as shown for the carmovirus turnip crinkle virus (TCV) (Stupina et al., 2011). For the umbravirus pea enation mosaic virus (PEMV), which contains three 3'-CITEs, direct and indirect modes were proposed to occur (Gao et al., 2012, 2013, 2014).

The carmovirus MNSV, which lacks a 3'-poly(A) tail and a 5'-cap (Díaz et al., 2003, 2004), controls its cap-independent translation with an ISS 3'-CITE named Ma5TE (Miras et al., 2017b). This 3'-CITE, with its 45 nucleotides (nt), is the shortest one known to date and consists of a stem that is closed with an apical 7 nt loop and interrupted by two internal loops that are 3 and 7 nt in length. Translation requires the presence of the 5'-UTR from MNSV *in cis* (Truniger et al., 2008). In addition to the genetic evidence that indicates that MNSV translation is eIF4E-dependent (Nieto et al., 2006; Rodríguez-Hernández et al., 2012), a direct interaction between its Ma5TE and eIF4F has recently been shown (Miras et al., 2017b). Mutations in eIF4E affect its association with eIF4G, reducing Ma5TE activity, thereby showing that both subunits of the eIF4F complex are important. Here we study how this translation initiation complex, which is bound to the Ma5TE, reaches the vicinity of the start codon. We have determined the secondary structure of the 5'-end of the MNSV genome, formed by 5 stem-loops (SL), and identified that the nucleotides from two loops are complementary to the apical loop of the 3'-CITE. Our experimental studies on the cooperation between these sequences show that interaction based on sequence complementarity between at least one of the 5'-end sequences and the 3'-CITE is required for some cap-independent translation of MNSV *in vivo*, but that both 5'-3' interactions are necessary for efficient translation and thus for wild-type virus multiplication.

MATERIALS AND METHODS

Analysis of RNA Structures

The 84 nt-long 5'-UTR of MNSV, and the 132 nt-long extended sequence of its 5'-end were cloned into a previously described SHAPE cassette plasmid (Wang et al., 2010). This plasmid was linearized with *Sma*I and transcribed using the MEGAscript™ Kit (Ambion). Selective 2'-Hydroxyl Acylation analyzed by Primer Extension (SHAPE) experiments using benzoyl cyanide (BzCN) were performed essentially as previously reported (Kraft et al., 2013; Miras et al., 2015). Briefly, 500 ng of RNA refolded in the SHAPE buffer (100 mM KCl, 50 mM HEPES KOH pH7.5, 8 mM MgCl₂) was treated with 60 mM BzCN (Sigma-Aldrich) for 30 s at 22°C in the absence or presence

of Mg^{2+} (0.1, 1, and 4 mM) and resolved on an 8% denaturing polyacrylamide-urea gel after primer extension with a ^{32}P -labeled primer complementary to the SHAPE cassette. Normalized BzCN reactivity values for each nucleotide position were calculated by SAFA Footprinting Software (Das et al., 2005). The RNA's secondary structure was determined with the MC-Fold computer program (Parisien and Major, 2008) using SHAPE reactivity data.

Secondary structure predictions of 5'- and 3'-ends of other viruses from the family *Tombusviridae* were performed with Mfold¹ or RNAalifold². The prediction of possible RNA interactions including the estimation of their statistical significance was obtained using the Transat web server³ (Wiebe and Meyer, 2010). For this, the 5'-end sequence was fused to the 3'-CITE or 3'-UTR sequence, separated by a track of 10 adenosines as described by Diaz-Toledano et al. (2017).

Reporter Constructs for *in Vivo* Translation Efficiency Assays

5'-UTR deletion mutants were created by PCR amplification (High fidelity system, ROCHE⁴) from the constructs 5'-UTR-luc or 5'-end-luc of MNSV-M α 5 (*luc* = Firefly luciferase gene), followed by directional cloning of the amplified fragment into the *KpnI/XbaI* sites of the luc-3'-UTR-M α 5 plasmid (Truniger et al., 2008). The forward primer started with sequence inside the 5'-UTR, including the T7 promoter sequence and *KpnI* restriction site, and the reverse primer was complementary to the 3'-end of the *luc* gene followed by *XbaI* [Δ SL 1 (Δ 21 nt), Δ SL 1+2 (Δ 51 nt) or SL1-3 (Δ 73 nt)]. The 3'-UTR deletion mutants were created by PCR amplification from luc-3'-UTR-M α 5 (Truniger et al., 2008), followed by directional cloning into the *XbaI/HpaI* sites of the 5'-UTR-M α 5-luc plasmid. The primer pairs used contained the sequence of the 5'-end of the 3'-UTR preceded by an *XbaI* site (forward) and the reverse sequence inside the 3'-UTR (Δ SL A = Δ 43 nt or Δ SL A+B = Δ 85 nt of 3'-UTR-M α 5) followed by a *HpaI* site. The 5'-end-luc-3'-UTR construct was obtained by cloning the first 132 nt of the MNSV-M α 5 genome into the *KpnI/NcoI* sites of the luc-3'-UTR-M α 5 plasmid. In this construct, the ATG of MNSV-ORF1 was in frame with the *luc* gene. Thus, to avoid luciferase synthesis from this start codon, it was mutated by site-directed mutagenesis from ATG to GTG resulting in a 5'-end-luc-3'-UTR. Site-directed mutagenesis on both UTRs and 5'-end was performed by amplification of plasmids 5'-UTR-luc-3'-UTR or 5'-end-luc-3'-UTR of MNSV-M α 5 (Truniger et al., 2008) using Pyrobest polymerase⁵ (Takara Bio Inc.) with primers (sense and antisense) containing the desired mutation followed by *DpnI* digestion to remove the input plasmid [see *in vitro* mutagenesis protocol (Sambrook and Russell, 2001)]. The deletion of Ma5TE* was obtained following the same method and using PCR amplification primers flanking the deletion. All constructs were verified by sequencing. The *BsmI*-linearized

plasmids were transcribed *in vitro* in the absence or presence of a cap analog (Promega) using the RiboMaxTM transcriptase (Promega⁶). 3'-CITE+K (wt and mutants) was added to the 5'-UTR-luc (wt and mutants) by PCR using a primer including the reverse sequence of the end of the *luc* gene plus the 3'-CITE (45 nt) sequence including the sequence added as a clamp, as described by Miras et al. (2017b).

In Vivo Translation Efficiency Assays

In vivo translation in melon protoplasts was assayed as described before (Truniger et al., 2008) measuring luciferase activity 4 h after electroporation of the RNA. These experiments were carried out at least four times for each construct. The *in vivo* translation efficiencies of the RNA constructs were analyzed in the presence and absence of the cap (obtained by *in vitro* transcription). The translation efficiencies of the capped RNA constructs were all similar, independently if the UTRs were wild-type or contained mutations. When indicated, hippuristanol (10, 30, 100, 300, and 1000 nM) was added to protoplasts directly after electroporation and kept during incubation. The stability of the assayed RNA constructs in melon protoplasts was assessed by Northern blot analysis of total RNA extracted at 0/2/4 h after electroporation from protoplast samples (after exhaustive washing) using a digoxigenin-labelled luciferase specific cRNA probe. The stability in protoplasts of all the mutant RNA constructs in protoplasts was found to be unchanged as compared to the wild-type constructs, independent of its translation efficiency (not shown).

Construction and Analysis of MNSV Virus Mutants

The mutations were introduced into the infectious clone pTOPO-MNSV-M α 5 (Diaz et al., 2004). The complete plasmids were PCR-amplified using Pyrobest polymerase (Takara) with primers containing the mutation. They were digested with *DpnI* to select for the mutant plasmids (Sambrook and Russell, 2001). All constructs were verified by sequencing. The ability of the *in vitro*-transcribed uncapped viral RNAs to multiply in protoplasts of susceptible melon was studied by Northern blot using a digoxigenin-labeled cRNA probe against the 3'-UTR of the MNSV-M α 5 genome (Diaz et al., 2004). Mutations G124C and C125G, located in ORF1, resulted in the change from Ala to Pro and Gly, respectively. But the results obtained allowed for concluding that these amino acid changes did not affect replicase activity, as the mutant viruses with the restored sequence complementarity were able to multiply with similar efficiency as wild-type MNSV-M α 5. The 3'-UTR of the progenies was amplified with MNSV-specific primers by RT-PCR (Roche) and sequenced. The 5'-UTR sequences of the progenies were determined by 5'-RACE using an MNSV-specific primer with sequence complementary to the second ORF and Moloney Murine Leukemia Virus RT (PrimeScriptTM Reverse Transcriptase, Takara) followed by PCR amplification (PrimeStar[®] HS DNA Polymerase, Takara). PCR was performed using the primer used for the reverse transcription and a primer

¹<http://unafold.rna.albany.edu/?q=mfold/RNA-Folding-Form>

²<http://rna.tbi.univie.ac.at/cgi-bin/RNAWebSuite/RNAalifold.cgi>

³<http://www.e-rna.org/transat/>

⁴<http://www.roche.com/index.htm>

⁵<http://www.takara-bio.com/>

⁶<http://www.promega.com/>

complementary to the first 10 nt of the MNSV genome containing four additional guanosine nucleotides at its 5'-end. The amplified fragment was sequenced. The mutations were stable in the progeny.

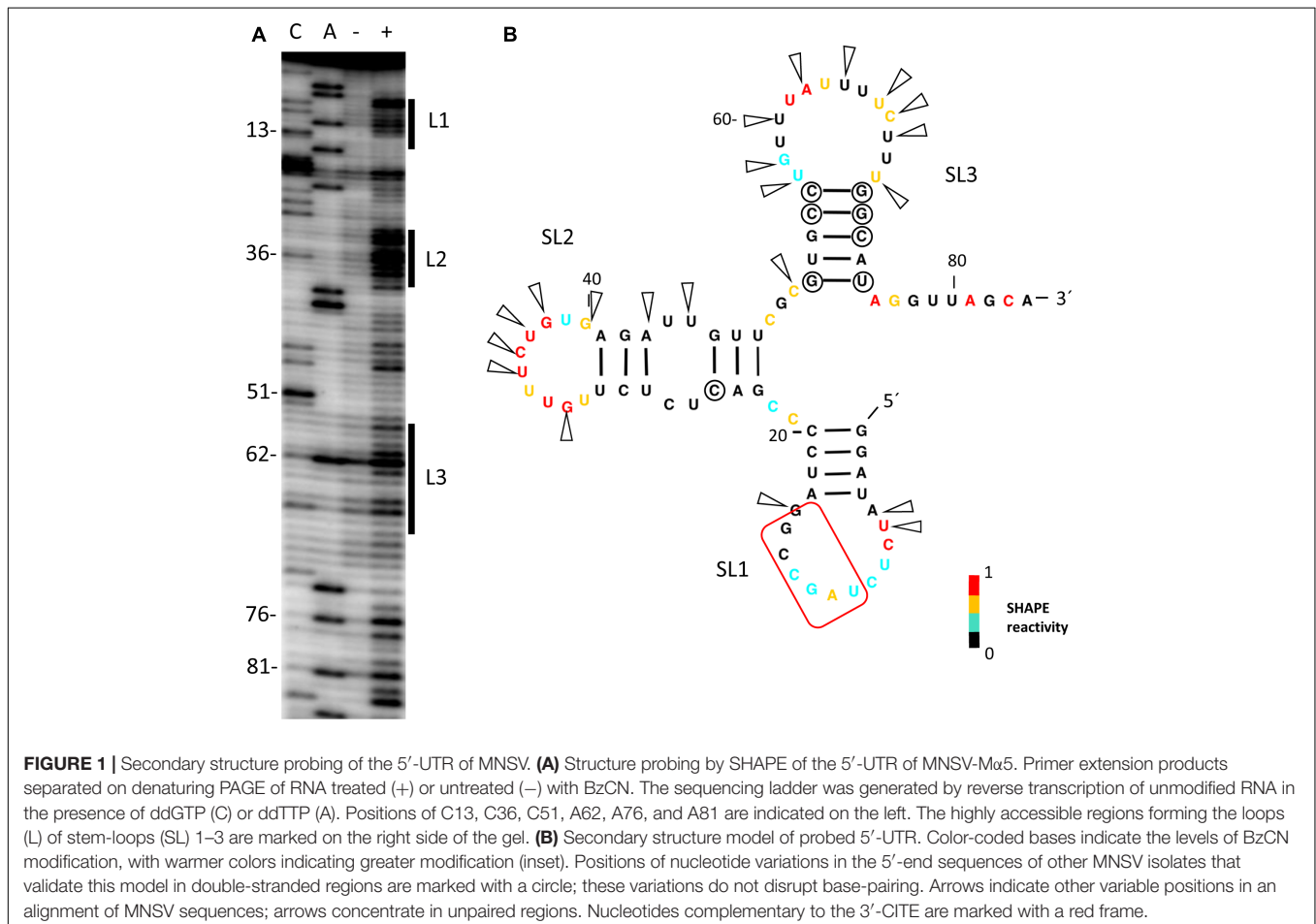
RESULTS

Analysis of the Secondary Structure of the 5'-UTR of MNSV and Importance of Its Regions in Cap-Independent Translation

Our previous experiments had shown that cap-independent translation of the MNSV isolate MNSV-M α 5 was controlled by its Ma5TE, the translation enhancer present in nearly all the MNSV isolates, and dependent on the presence of the 5'-UTR *in cis* (Truniger et al., 2008; Miras et al., 2017b). Thus, we studied the secondary structure from the 5'-UTR of the MNSV-M α 5 RNA genome by Selective 2'-Hydroxyl Acylation analyzed by Primer Extension (SHAPE) using the chemical benzoyl cyanide (BzCN), which modifies accessible nucleotides in a sequence-independent manner in seconds, forming 2'-O-adducts that block reverse transcriptase (Mortimer and Weeks, 2008). Primer extension

revealed three exposed regions (L1–L3) modified by BzCN, corresponding to the loops of the three stem-loop structures (SL) (Figure 1). Magnesium titration experiments showed that 5'-UTR folding was independent of this divalent cation (data not shown). Most variations in the 5'-UTR sequences of the MNSV isolates present in GenBank either do not disrupt base-pairing of double-stranded regions (circles in Figure 1B), or are preferentially localized in single-stranded regions (arrowheads). This sequence conservation supports the secondary structure model.

To identify the regions of the 5'-UTR of MNSV-M α 5 that are important for translation, we studied the effect of deletions of the SL1–3 found in this UTR (total length 84 nt) when flanking the luciferase gene (5'-UTR-luc-3'-UTR) on cap-independent translation in melon protoplasts (Truniger et al., 2008). The results obtained in the *in vivo* translation experiments of melon protoplasts showed that deletion of the first 21 nt corresponding to SL1 and thus, both other deletions [SL1+2 (Δ 51) and SL1+2+3 (Δ 73)] as well, strongly affected the cap-independent translation efficiency of the constructs (Figure 2A), suggesting that these first nucleotides were critical for Ma5TE activity. Also the apical small SL of the Ma5TE (Figure 2B), defined previously (Miras et al., 2017b), was shown to be critical for its activity.



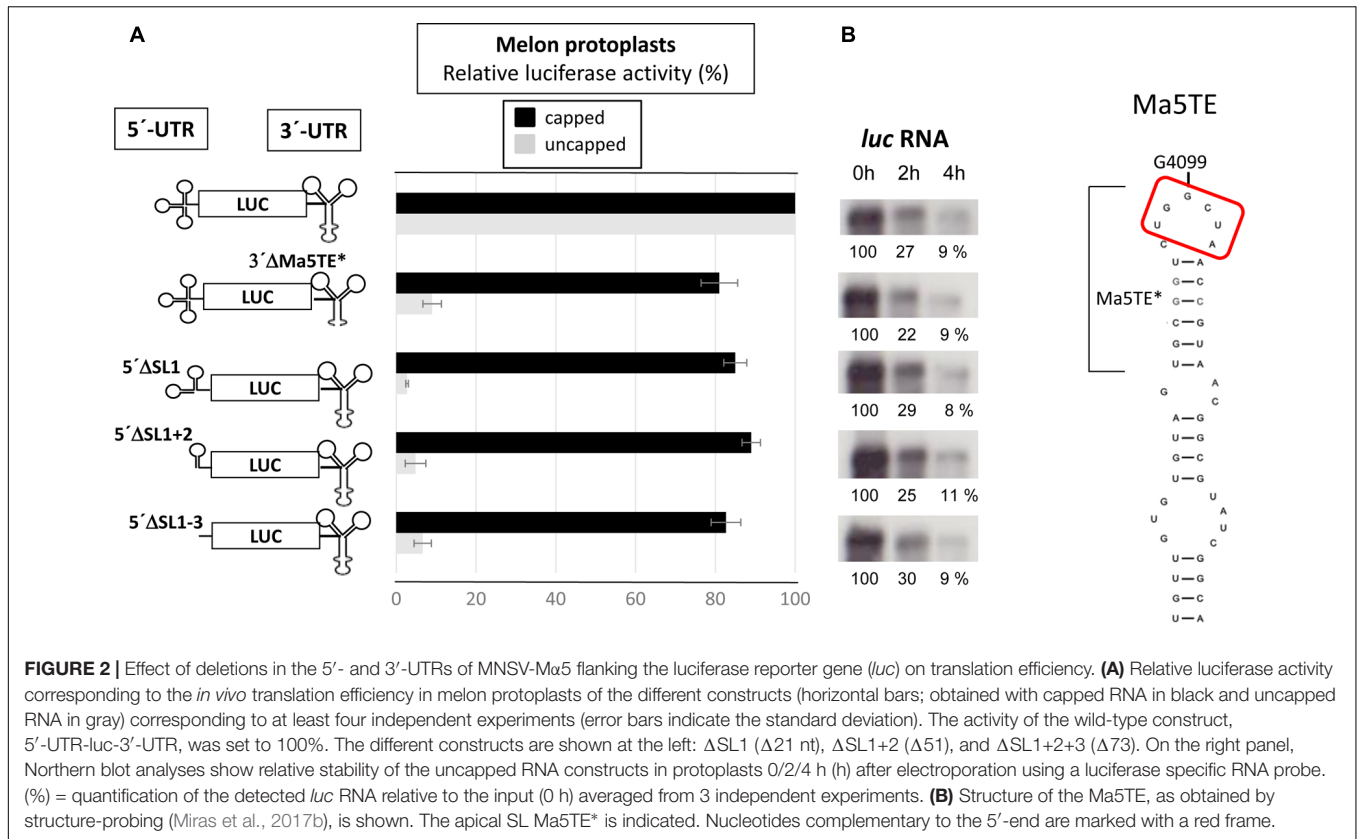


FIGURE 2 | Effect of deletions in the 5'- and 3'-UTRs of MNSV-Mα5 flanking the luciferase reporter gene (*luc*) on translation efficiency. **(A)** Relative luciferase activity corresponding to the *in vivo* translation efficiency in melon protoplasts of the different constructs (horizontal bars; obtained with capped RNA in black and uncapped RNA in gray) corresponding to at least four independent experiments (error bars indicate the standard deviation). The activity of the wild-type construct, 5'-UTR-*luc*-3'-UTR, was set to 100%. The different constructs are shown at the left: ΔSL1 (Δ21 nt), ΔSL1+2 (Δ51), and ΔSL1+2+3 (Δ73). On the right panel, Northern blot analyses show relative stability of the uncapped RNA constructs in protoplasts 0/2/4 h (h) after electroporation using a luciferase specific RNA probe. (%) = quantification of the detected *luc* RNA relative to the input (0 h) averaged from 3 independent experiments. **(B)** Structure of the Ma5TE, as obtained by structure-probing (Miras et al., 2017b), is shown. The apical SL Ma5TE* is indicated. Nucleotides complementary to the 5'-end are marked with a red frame.

Importance of Sequence Complementarity Between Both UTRs of MNSV-Mα5 for the *in Vivo* Translation Efficiency of *luc*-Constructs

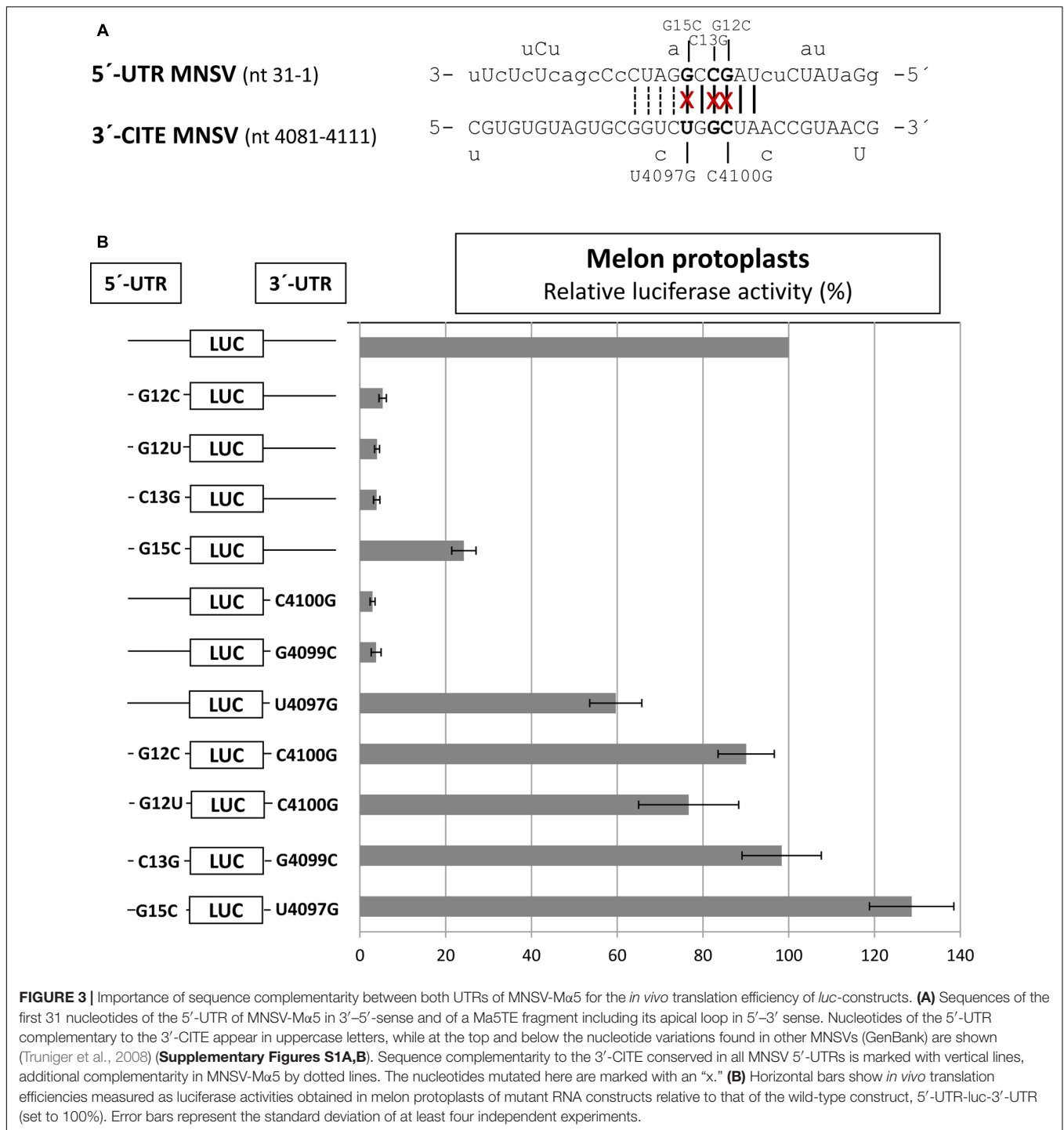
By comparing the sequences of the first 21 nt of MNSV with that of its 3'-CITE, six complementary nucleotides that were invariant in the genomes of the MNSV isolates available in GenBank (Supplementary Figure S1), could be identified. These complementary nucleotides were present in loops in the secondary structures assayed, in SL1 of the 5'-UTR (Figure 1B) and in the apical loop of the 3'-CITE (Figure 2A). Complementarity could be extended from 6 to 10 nucleotides for MNSV-Mα5 (Figure 3A). To study the possibility of a direct 5'-3' interaction based on nucleotide complementarity, we exchanged single nucleotides from the loop of SL1 (G12C, G12U, C13G, and G15C) and the corresponding complementary nucleotides from the 3'-CITE (C4100G, G4099C, and U4097G) in the 5'-UTR-*luc*-3'-UTR construct (Truniger et al., 2008) (Figure 3A). We studied the effects of these mutations on the *in vivo* cap-independent translation efficiency. These analyses showed that each of the single point mutations in the 5'- or 3'-UTR caused a strong reduction in the translation efficiency of the construct, resulting in less than 10% of the luciferase activity obtained with the wild-type construct (Figure 3B). Mutations G15C and U4097G caused smaller reductions, approximately 30 and 60% of the luciferase activity obtained with the wild-type construct, respectively. Importantly, the

introduction of the complementary mutations (G12C/C4100G, G12U/C4100G, C13G/G4099C, and G15C/U4097G) restored the translational activity to levels similar to those shown by the wild-type construct. The fact that both G12C and G12U mutations were able to compensate C4100G, confirmed that sequence complementarity between both UTRs was important for cap-independent translation controlled by the Ma5TE. Additionally, the fact that the translation efficiency of the G12U/C4100G construct was lower than that of the wild-type and the G12C/C4100G constructs, suggests that the weaker U-G interaction leads to reduced translation. In line with this result, the stronger C-G interaction of the G15C/U4097G construct resulted in a higher translation efficiency than the wild-type construct.

In agreement with this notion, for the ISS of MNesV, it has been shown that an interaction based on sequence complementarity between the nucleotides of the apical loop of the ISS and the first loop in the predicted CIRV 5'-UTR structure was required for 3'-CITE activity (Nicholson et al., 2010).

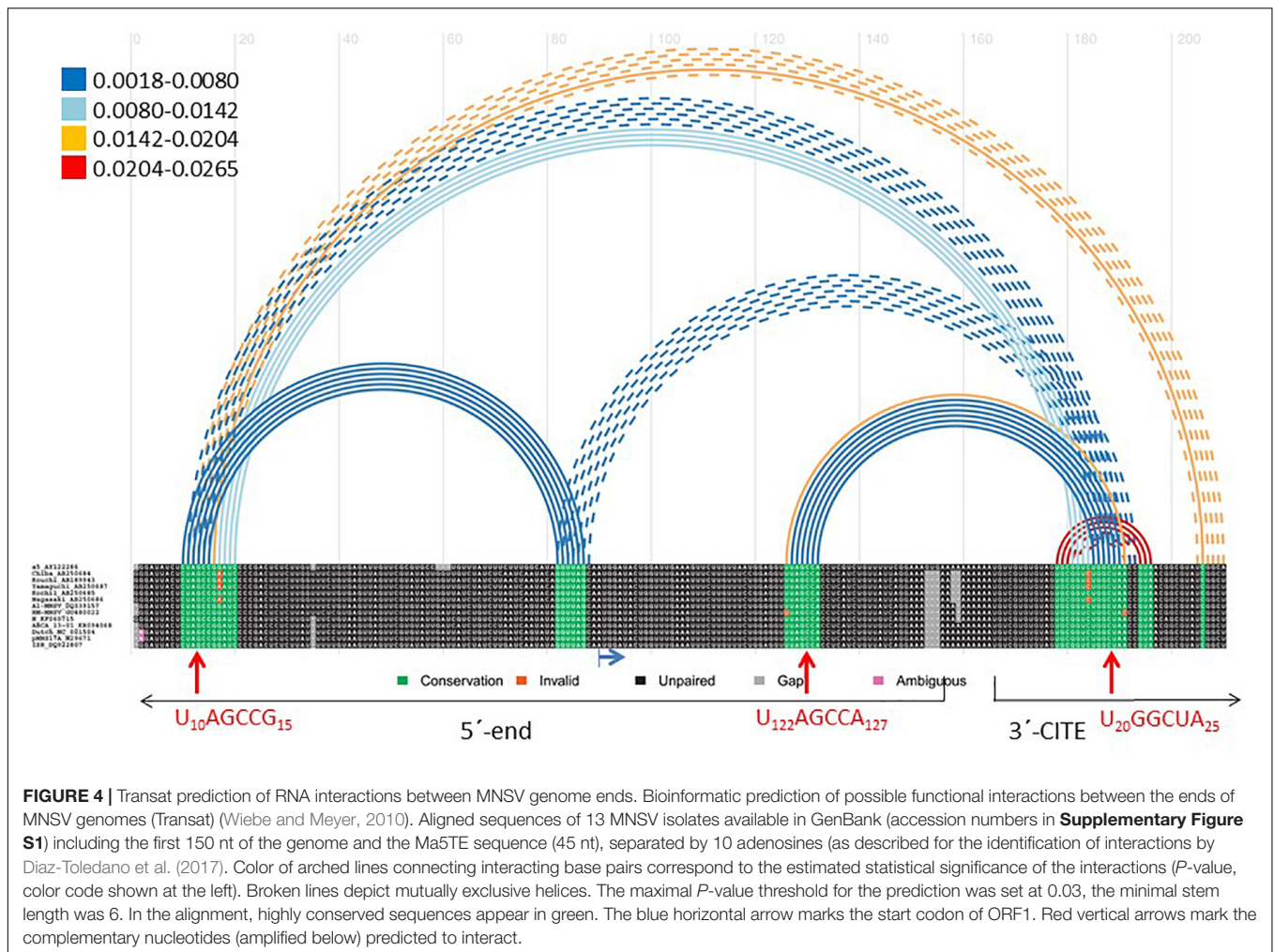
Prediction of Additional RNA Interactions Between the Ends of MNSV Genomes

We used the Transat bioinformatics tool, that detects conserved helices of high statistical significance, including pseudo-knotted, transient and alternative structures starting with a multiple sequence alignment (Wiebe and Meyer, 2010), to predict interactions between the ends of MNSV genomes. Here, we



used an alignment of the 5'-ends (including the first 150 nt) and the nearly invariant 3'-CITEs (45 nt) of the MNSV genomes (see **Supplementary Figure S1**). The program predicted the interaction between the apical loop of the Ma5TE (U20–A25) and the six nucleotides of the 5'-UTR (U10–G15) that we had identified to be important for translation (**Figure 4**). Additionally, the tool also predicted an interaction between the same nucleotides of the Ma5TE and the six nucleotides located

in ORF1, U122–A127 (red arrows). Both 5'-3' interactions were predicted with high statistical significance (**Figure 4**), also when the analysis was performed with the complete 3'-UTR (**Supplementary Figure S2**). Previously, it had been suggested that the sequence present in ORF1 could possibly play a role in 5'-3' interaction (Simon, 2015). Transat also predicted another dual interaction with high statistical significance (**Figure 4**), between G77–G82 and C9–C14 or C4100–C4106, but our assayed

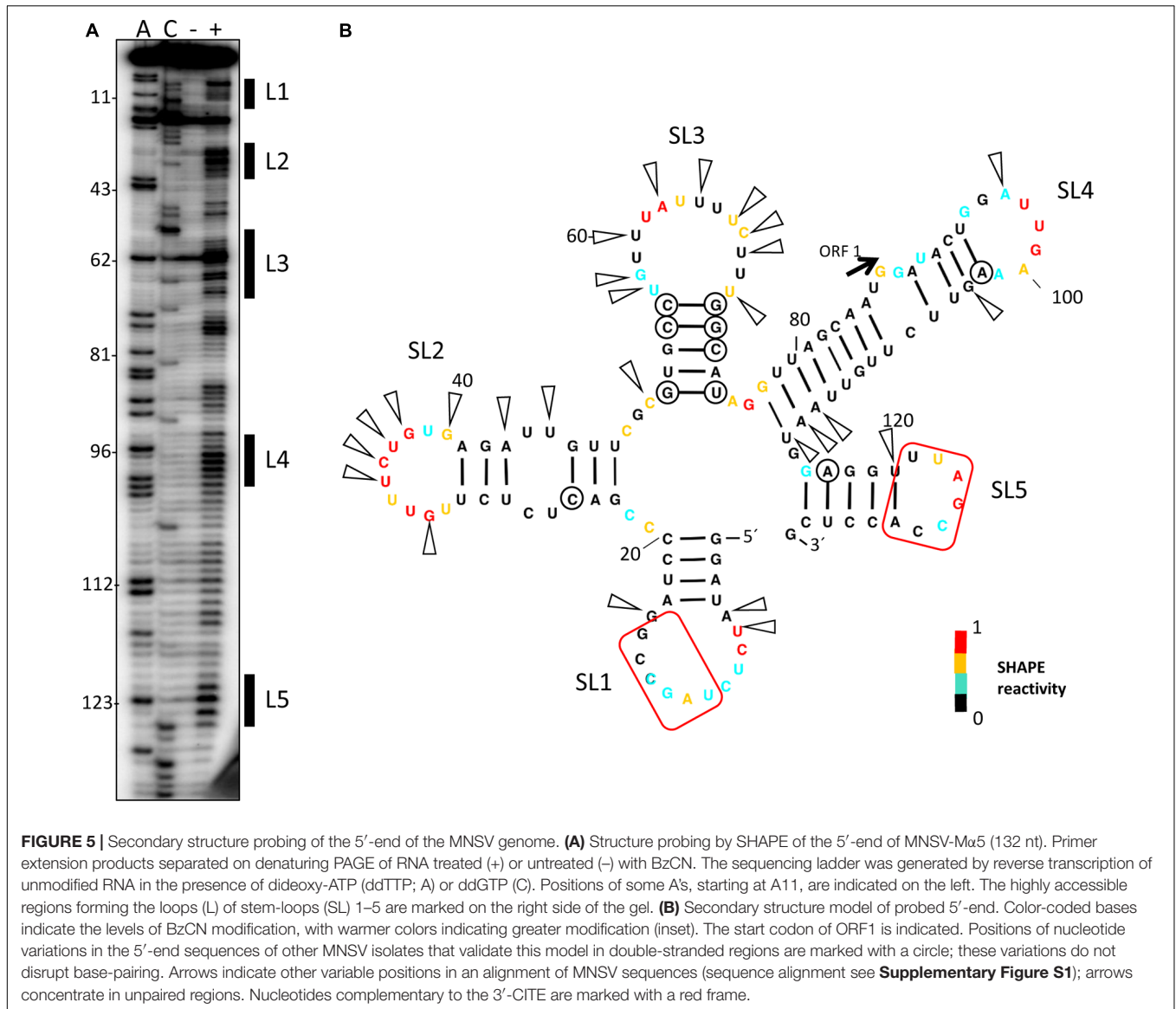


5'-end (Figure 5) and Ma5TE (Figure 2B) RNA structures did not support this prediction, as part of the nucleotides involved were present in stems. But the possibility that these predicted interactions are transient and dynamic cannot be excluded.

To study the possible importance of the predicted interaction between nucleotides located in ORF1, U122–A127, and the Ma5TE, we first examined the secondary structure of the 5'-end of the MNSV-Mα5 RNA genome with SHAPE (Figure 5). The first three SLs coincided with the UTR structure (Figure 1). The ORF1 sequence (from nt 121–127), complementary to the Ma5TE, was located in the SL5 loop. Thus, as it was unpaired, it may be involved in an interaction, based on sequence complementarity. Additionally, the alignment of the 5'-end and 3'-CITE sequences of the MNSV genomes present in GenBank showed that the complementary sequence stretches in the UTRs and in ORF1 were invariant in all MNSV isolates (Supplementary Figure S1) (Truniger et al., 2008; Miras et al., 2017b), supporting their importance. Thus, interaction of the 3'-CITE with the 5'-UTR seemed to be a general mechanism in MNSV translation, but an additional interaction with ORF1 could still exist.

Importance of the Complementary Sequence Stretch in ORF1 in Ma5TE-Controlled Cap-Independent Translation

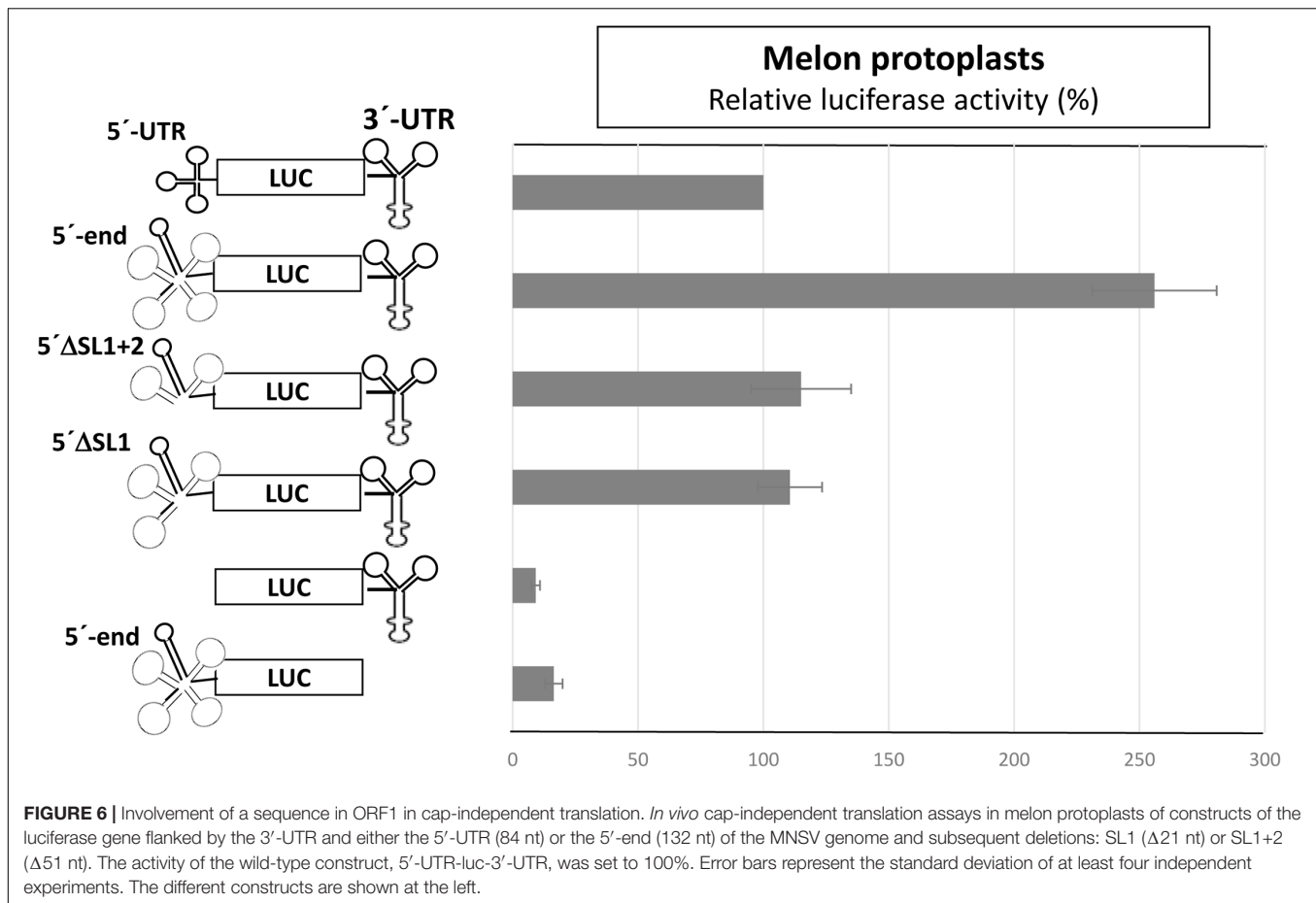
To analyze whether the complementarity between Ma5TE and both 5'-end sequence stretches was important for Ma5TE-mediated cap-independent translation, we added part of ORF1 (48 nt) to the 5'-UTR of MNSV-Mα5, flanking the *luc* gene (5'-end-*luc*-3'-UTR). Since the AUG from MNSV-ORF1 was in frame with the *luc* gene and to avoid luciferase synthesis from this start codon, it was mutated by site-directed mutagenesis from AUG to GUG, resulting in the 5'-end-*luc*-3'-UTR. In this work we differentiate between the genomic 5'-UTR (untranslated sequence) and the 5'-end, including additionally sequence downstream from the start codon. The cap-independent translation activity in melon protoplasts of the previous 5'-UTR-*luc*-3'-UTR construct was 2.5-fold lower than that of the new one (Figure 6, first and second bars), suggesting that the added sequence played a role in translation. Additionally, the deletion of SL1 or SL1+2 of the 5'-end-*luc*-3'-UTR constructs reduced the translation efficiencies only to levels similar to that



of the UTR-construct (**Figure 6**, third and fourth bars) and not less than 10% as shown in **Figure 2**. Thus, the added sequence seemed to be able to compensate for the loss of the 5'-UTR-3'-CITE interaction of the deletion constructs, suggesting that it could contain a second 3'-CITE-interacting sequence that is important for efficient *in vivo* cap-independent translation.

Thus, we studied the effect of point mutations in the 5'-end nucleotides complementary to the same Ma5TE sequence using the 5'-end-luc-3'-UTR construct, disrupting one or both possible complementary interactions (**Figure 7A**). The luciferase activities obtained *in vivo* with these wild-type and mutant RNAs (**Figure 7B**) revealed that single point mutations in one of the two sequence stretches of the 5'-end (C13G, C125G, G12C, and G124C) reduced the translation efficiency to 20–50% of the wild-type activity, while reduction was much stronger for the constructs with the single mutations in the 3'-CITE or the double mutations in the 5'-end (approximately 10%

of the wild-type activity; G4099C, C4100G, C13G/C125G, and G12C/G124C). In these constructs, both possible complementary 5'-3' interactions were disrupted, explaining the low translation efficiency. In agreement with this view, restoring the nucleotide complementarity between the mutated Ma5TE and one of the two 5'-end sequences led to a partial recovery of the translation efficiency (C13G-G4099C, C125G-G4099C), and only the restoring of the nucleotide complementarity with both 5'-end sequences (CCG = C13G, C125G- plus G4099C) led to its complete recovery. The results obtained with the constructs, including mutation C4100G [G12C-C4100G, G124C-C4100G and GGC (=G12C, G124C plus C4100G)] also support this explanation, although the translation percentages with respect to the wild-type construct were higher, maybe due to the change of C4100 into G was of some advantage for Ma5TE activity or because G–G mismatches have been shown to be more stable than the C–C mismatches (Kierzek et al., 1999). These



results suggest that both complementary sequences in the 5'-end are necessary for highly efficient Ma5TE-mediated cap-independent translation *in vivo*, while complementarity with at least one of the 5'-end sequences is required for Ma5TE activity. The mutational analysis was repeated with 5'-end-luc-3'-CITE constructs (Supplementary Figure S3), with the 3'-UTR exchanged in just the Ma5TE. Similar results were obtained, confirming that this dual interaction was only Ma5TE-dependent and independent from the rest of the 3'-UTR.

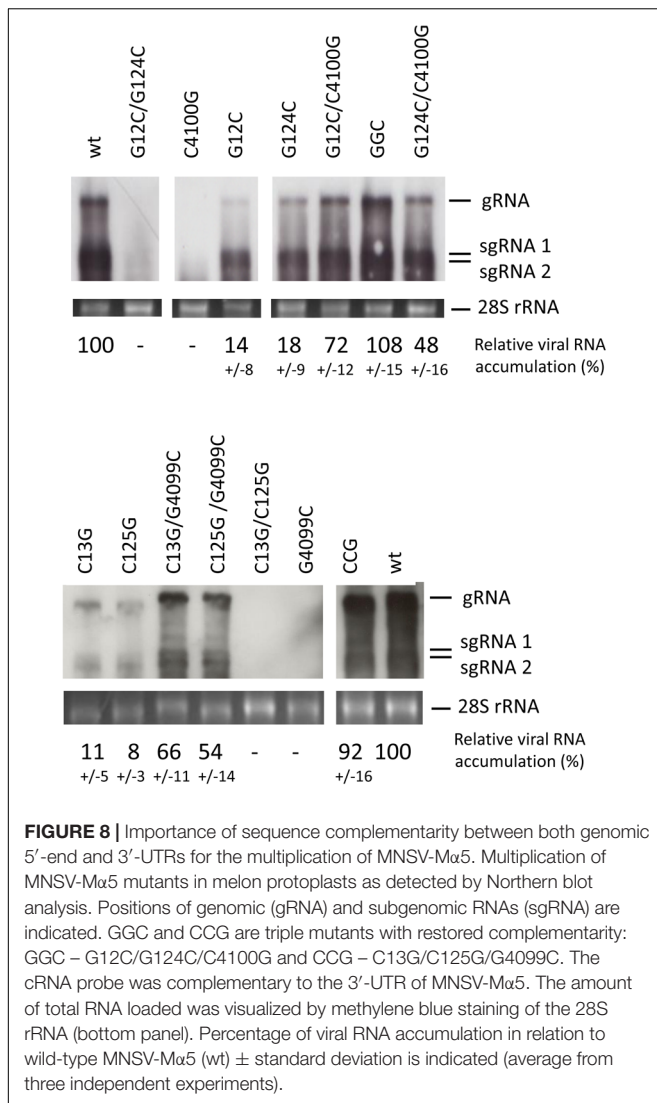
Importance of Sequence Complementarity Between Both Ends of the MNSV-M α 5 Genome for Virus Multiplication

The results obtained above with the reporter constructs and the high conservation of this dual sequence complementarity in the genomes of different MNSV isolates (Supplementary Figure S1) suggested that these interactions could be important for virus multiplication. Thus, we studied the effect of partial or total loss of the sequence complementarities identified above on the MNSV-M α 5 genome multiplication capacity in melon protoplasts. As shown in the Northern blots in Figure 8, mutant viruses with both complementary interactions disrupted (with a single point mutation in the Ma5TE sequence or with mutations

in both complementary 5-end sequence stretches) were unable to multiply in melon protoplasts (G12C/G124C, C4100G, C13G/C125G, and G4099C), correlating with the negative effect of these mutations on the translation efficiency observed in the previous experiments. On the other hand, disruption of only one of the complementary sequence interactions by single mutations on the 5'-end allowed some virus multiplication (G12C, G124C, C13G, and C125G). In the presence of the corresponding complementary mutation in the Ma5TE, virus multiplication was higher (G12C/C4100G, G124C/C4100G, C13G/G4099C, and C125G/G4099C), but only when sequence complementarity between both sequence stretches was restored (GGC, CCG) did virus multiplication reach wild-type levels. Thus, in agreement with the previous results, both complementary interactions seemed to be required for wild-type multiplication efficiency.

Additional Factors That Are Important for Cap-Independent Translation Controlled by the M α 5TE

Ribosome scanning occurs from the 5'-end of the viral genome in several cases of 3'-CITE-mediated translation, as shown for BTE (Guo et al., 2001). In that case, addition of a sequence stretch that folds into a stable SL at the 5'-end has been shown to avoid ribosome loading, inhibiting BTE-mediated translation.



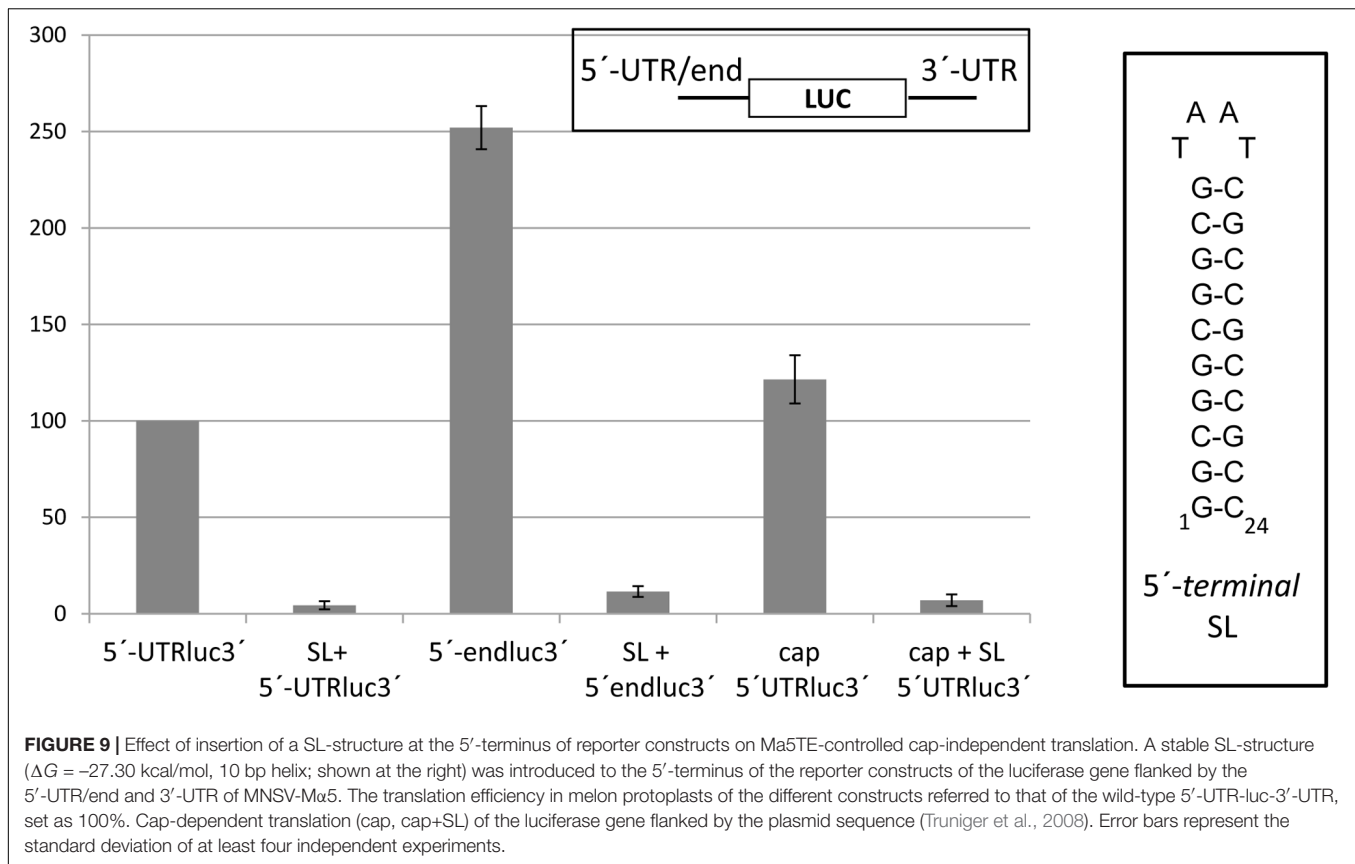
maintenance of at least one of these interactions is essential for translation and multiplication. These complementary sequence stretches are invariant in all MNSV isolates, suggesting that these dual interactions between both genome ends are a general mechanism required for cap-independent translation and multiplication of MNSVs.

To learn if these dual 5'-3' interactions could be predicted to be a more general mechanism of carmoviruses or viruses with ISS, we analyzed their 5'-end and 3'-CITE sequences. For these viruses, 5'-end interactions based on sequence complementarity with their 3'-CITEs have been shown or proposed to reside either in the vicinity of the first SL of the predicted 5'-UTR structure or within the first ORF (Simon and Miller, 2013). We could identify in all cases of viruses with ISS and some carmoviruses sequence stretches containing five or more nucleotides complementary to the 3'-CITE loop in both the 5'-UTR and ORF1 (**Supplementary Tables S1, S2**). The nucleotides involved were mostly unpaired in the predictions (with Mfold) of the 5'-end secondary structure of these virus genomes, and could therefore possibly be involved

in an interaction with its 3'-CITE (**Supplementary Figure S4**). Out of these viruses, only for carnation mottle virus (CarMV), enough sequenced isolates exist in GenBank for performing the bioinformatic analysis for predicting RNA interactions using Transat. Interestingly, also for this virus a dual interaction could be predicted (**Supplementary Figure S5**). Thus, such dual interactions may also exist in other viruses of the family *Tombusviridae* (containing different 3'-CITEs). But to draw any conclusions, this interaction should first be studied in detail in each virus.

With regards to the 5'-3' interactions based on sequence complementarity proposed for other viruses with 3'-CITEs, some of the published experimental results could be explained with this dual interaction: for example, for the YSS of the tombusvirus CIRV, a 5'-UTR-3'-CITE interaction has been shown to exist, but mutations in the complementary sequence of the YSS reduced virus multiplication much more than mutations in the 5'-UTR, and restoring complementarity in the 5'-UTR mutant did not result in increased virus multiplication (Nicholson and White, 2008). The authors explain these results with the higher stability of the G-G versus the C-C mismatch, but the presence of a second 5'-3' interaction required for efficient translation activity, as described here for MNSV, could also provide an additional explanation. Also for this tombusvirus, a second complementary 6 nt sequence stretch located in ORF1 (nt 152–157) was identified, apart from the one found in the 5'-UTR (nt 18–22). In the Mfold RNA structure prediction of the CIRV 5'-end these complementary sequence stretches were unpaired (**Supplementary Figure S4C**) and, thus, they may interact with a complementary sequence. Also, in some other cases, the finding that single mutations in the 5'-end of the predicted 5'-3'-interacting sequence stretches only had a slight negative effect on virus translation, while the introduction of the complementary mutation in the opposite end did not restore translation to wild-type levels, may indicate that dual interactions are involved in efficient cap-independent translation (Meulewaeter et al., 1998a,b; Guo et al., 2001; Sarawaneeyaruk et al., 2009). On the other hand, experimental results obtained for SCV (Chattopadhyay et al., 2011), TBSV (Fabian and White, 2004, 2006) and MNeSV (Nicholson et al., 2010) did not support such a dual interaction. The results for MNeSV were obtained with a chimeric CIRV virus, with its YSS exchanged with the ISS from MNeSV; thus, the identified 5'-3' interaction occurred between the ISS of MNeSV and the 5'-UTR of CIRV (Nicholson et al., 2010). In conclusion, to know if a dual interaction between both genome ends is a more general mechanism required in cap-independent translation, further studies are needed.

We have recently shown that the 3'-CITE of MNSV binds eIF4F through eIF4E (Miras et al., 2017b). The 5'-3' interactions identified in the present work could be responsible for bringing the translation initiation complex bound to the Ma5TE to the 5'-end of the genomic RNA. Since both 5'-end sequences are complementary to the same sequence of the 3'-CITE, these interactions should be mutually exclusive, and may occur one after the other. While the interaction of the Ma5TE with the two sequences of the 5'-end is required for efficient

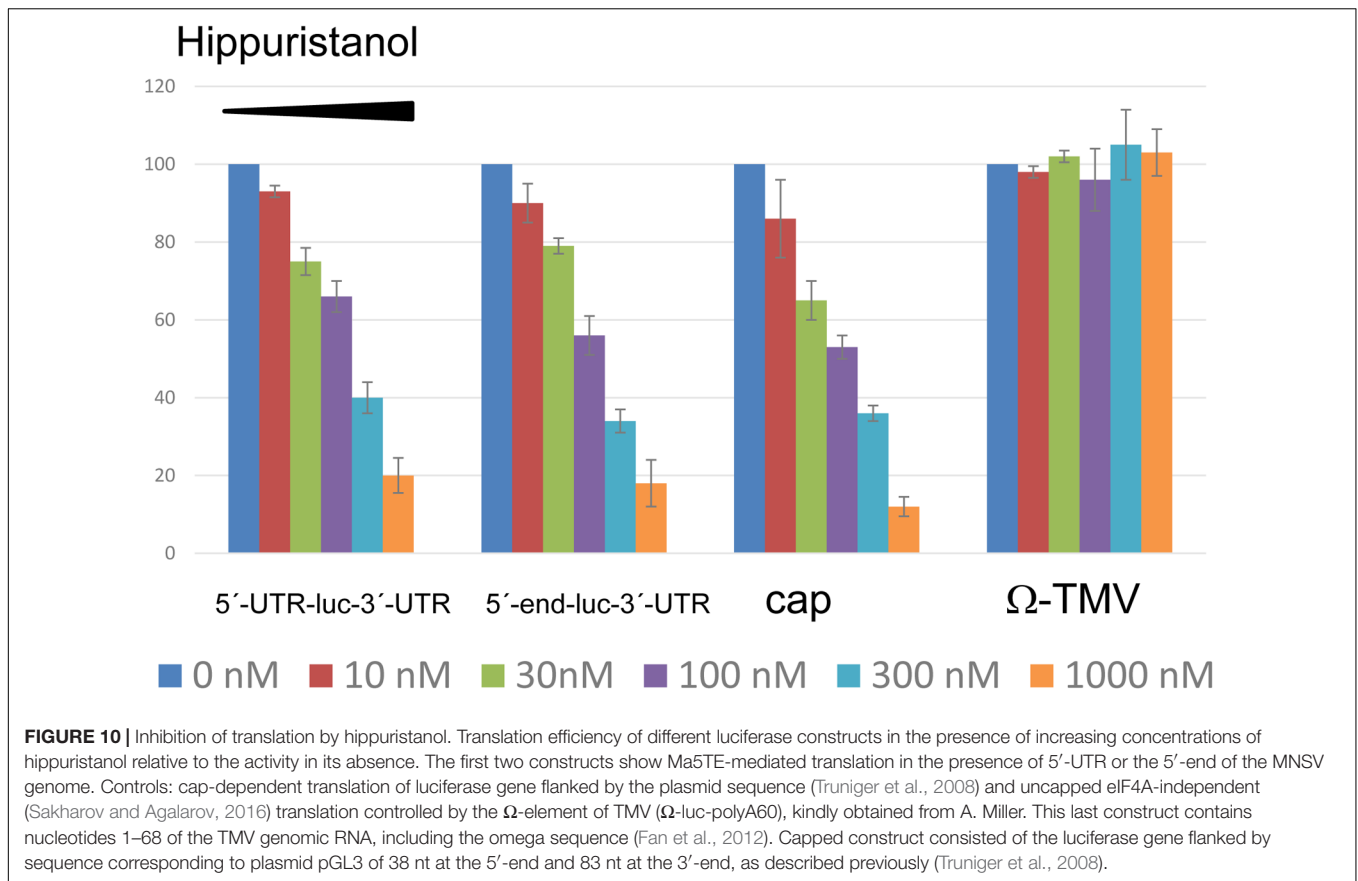


translation and virus multiplication, some translation still occurs if one of these interactions is missing and is only abolished if both interactions fail. Thus, although it is advantageous for virus RNA translation to have both connections, they are not essential. The translation efficiency could be increased when both connections are present, as their cooperative binding could help to keep the 3'-CITE in close proximity of the 5'-end. Thus, if one 5'-interaction is disrupted by the scanning or translating activity of the ribosome, the other could be binding the just freed 3'-CITE again. Additionally, we have observed that the secondary structure predictions of the 5'-UTR and the 5'-end of MNSV using RNAalifold (structural alignment using sequences from MNSV isolates available in GenBank) and Mfold differed from our probed structures (**Supplementary Figure S6** and **Figures 1B, 5**). The difference was in the first 22 nucleotides, which form SL1 in our probed structure. Thus, while in our probed structure the nucleotides interacting with the 3'-CITE were in the SL1 loop, in the structure prediction they appeared paired to the complementary sequence either at the 5'-UTR end or at the beginning of ORF1. If both conformations have a role and coexist in the genome, the dual interaction would be advantageous.

An example of two eIF4E-binding structures in the 5'-end of a mRNA has been described for the human histone H4-mRNA (Martin et al., 2011), which has a 5'-cap and also an eIF4E-sensitivity element (4E-SE) in the coding region. The cap-structure is hidden inside a secondary structure, which first

has to be melted by eIF4A to become accessible to eIF4E. Thus, the authors proposed that this helicase would be released to the 5'-end by the interaction of eIF4F through eIF4E with the 4E-SE, which would result in the melting of the secondary structure, freeing the 5'-cap. A mutant H4-mRNA with 4 nt changes in the 4E-SE showed a twofold lower translation efficiency than the wild-type H4-mRNA. A similar mechanism could be proposed for translation of the MNSV genome: although the interaction of the 3'-CITE with the ORF1 sequence is sufficient for translation, eIF4A could be released through this interaction and could melt the upstream secondary structure. In favor of this proposal, our results suggest that MNSV Ma5TE-driven translation is eIF4A-dependent, as previously shown only for another 3'-CITE, the one found in BYDV (Zhao et al., 2017). Also, our results suggest that the ribosome must be loaded at the 5'-terminus of the MNSV RNA, as previously shown for BYDV (Rakotondrafara et al., 2006), TBSV (Fabian and White, 2006) and for the chimeric CIRV/MNeSV virus (Nicholson et al., 2010). Dynamic RNA structures that play different roles have been recently described in other viral genomes (Kuhlmann et al., 2016; Liu et al., 2016; Romero-López and Berzal-Herranz, 2017).

It is often difficult to show 5'-3' RNA:RNA interactions experimentally: if they are transient or require proteins, these interactions may be difficult to detect biochemically. Also, if the interacting nucleotides have additional functions, no compensation will be observed by complementary mutations.



Our results of the *in vivo* compensatory mutational analysis clearly support the interactions between the 5'-end and 3'-CITE of MNSV-Mα5 based on sequence complementarity. But we were not able to show this interaction *in vitro*, neither with RNA transcripts of different lengths using gel retardation protocols that were successful for other RNA–RNA interactions (Fabian and White, 2006; Romero-López and Berzal-Herranz, 2009; Nicholson et al., 2010), nor performing atomic force microscopy (AFM) studies (Alvarez et al., 2005) to visualize circularization with the translationally active luciferase construct (data not shown). Thus, we propose that in this case, additional protein factors, possibly the translation initiation factors bound to the 3'-CITE, may stabilize this 5'–3' interaction. Also, in other cases it has been proposed that host protein(s) enhance base-pairing (Rakotondrafara et al., 2006), as found for the Norwalk virus (Sandoval-Jaime and Gutiérrez-Escolano, 2009). The *in vitro* formation of a tripartite complex of 5'-UTR-3'-CITE-eIF4E, which is required for efficient ribosome recruitment to the start codon, has been shown for MNeSV (Nicholson et al., 2010).

CONCLUSION

We show that at least one interaction based on sequence complementarity between the Ma5TE and the 5'-end of the MNSV RNA genome is essential for virus translation and

multiplication, but a second interaction is advantageous for these viral functions.

AUTHOR CONTRIBUTIONS

MM, AR-H, JC, and VT performed the experiments. MM, CR-L, JC, and VT analyzed the data. MA, MM, and VT conceived the study. MM, MA, CR-L, AB-H, and VT wrote the manuscript. All authors read and approved the final manuscript.

FUNDING

This work was supported by grants AGL2009-07552/AGR, AGL2015-72804-EXP, and AGL2015-65838 (MINECO, Spain) and 19252/PI/2014 (Fundación Seneca, Spain). AR-H was supported by grants from the National Council of Science and Technology (CONACyT, Mexico) and the Spanish Agency for International Development Cooperation (AECID). MM was recipient of a fellowship from the Spanish Ministerio de Ciencia e Innovación (BES-2010-032827).

ACKNOWLEDGMENTS

We thank J. Pelletier and R. Cencic for providing the hippuristanol. We thank A. Miller for providing the luciferase

construct including W-TMV leader. M. Fon checked the English (mariogfon@gmail.com). We acknowledge support of the publication fee by the CSIC Open Access Publication Support Initiative through its Unit of Information Resources for Research (URICI).

SUPPLEMENTARY MATERIAL

The Supplementary Material for this article can be found online at: <https://www.frontiersin.org/articles/10.3389/fpls.2018.00625/full#supplementary-material>

FIGURE S1 | Nucleotide sequence conservation of the 5'-end and 3'-CITE of MNSV genomes. **(A)** Sequence alignment of the 5'-end sequences of MNSV isolates using ClustalW. **(B)** Sequence alignment of the 3'-CITE sequences of MNSV isolates using ClustalW. The GenBank accession numbers of MNSV sequences included in the alignments are Mα5 (MNSV-Mα5)-AY122286, Ma71-EU589619, Ma24-EU589616, Pa58-EU589620, Chiba-AB250684, Kouchi-AB189943, Yamaguchi-AB250687, Kochi-AB250685, Nagasaki-AB250686, AI-DQ339157, HM-GU480022, ABCA-KR094068, N-KF060715, ISR-DQ922807, Dutch-NC001504, 264-AY330700, and 17A/01A-M29671. The nucleotides conserved in all the sequences are marked with an asterisk (*) below the aligned sequences. The complementary sequence stretches involved in the two 5'-3' interactions, as well as the ORF1 start codon, are boxed.

FIGURE S2 | Prediction of RNA interactions between the 5'-end and 3'-UTR of MNSV genomes. Bioinformatic prediction of possible functional interactions between the ends of MNSV genomes (Transat) (Wiebe and Meyer, 2010). Aligned sequences of 13 MNSV genomes (GenBank accession numbers in **Supplementary Figure S1**) including the first 150 nt and the 3'-UTR sequence, separated by 10 adenines. Color of arched lines connecting interacting base pairs correspond to the estimated statistical significance of the interactions (*P*-value, color code at the left). Broken line arcs depict mutually exclusive helices. The maximal *P*-value threshold for the prediction was set at 0.02, the minimal stem length was 6. Highly conserved sequences appear in green in the alignment. The blue horizontal arrow marks the start codon of ORF1. Red vertical arrows mark the complementary nucleotides (amplified below) predicted to interact.

REFERENCES

- Alvarez, D. E., Lodeiro, M. F., Luduena, S. J., Pietrasanta, L. I., and Gamarnik, A. V. (2005). Long-range RNA-RNA interactions circularize the dengue virus genome. *J. Virol.* 79, 6631–6643. doi: 10.1128/jvi.79.11.6631-6643.2005
- Batten, J. S., Desvoyes, B., Yamamura, Y., and Scholthof, K.-B. G. (2006). A translational enhancer element on the 3'-proximal end of the *Panicum mosaic virus* genome. *FEBS Lett.* 580, 2591–2597. doi: 10.1016/j.febslet.2006.04.006
- Blanco-Pérez, M., Pérez-Cañamás, M., Ruiz, L., and Hernández, C. (2016). Efficient translation of *Pelargonium line pattern virus* RNAs relies on a TED-like 3'-translational enhancer that communicates with the corresponding 5'-Region through a long-distance RNA-RNA interaction. *PLoS One* 11:e0152593. doi: 10.1371/journal.pone.0152593
- Cencic, R., and Pelletier, J. (2016). Hippuristanol - A potent steroid inhibitor of eukaryotic initiation factor 4A. *Translation* 4:e1137381. doi: 10.1080/21690731.2015.1137381
- Chattopadhyay, M., Shi, K., Yuan, X., and Simon, A. E. (2011). Long-distance kissing loop interactions between a 3' proximal Y-shaped structure and apical loops of 5' hairpins enhance translation of Saguaro cactus virus. *Virology* 417, 113–125. doi: 10.1016/j.virol.2011.05.007
- Chkuaseli, T., Newburn, L. R., Bakhshinyan, D., and White, K. A. (2015). Protein expression strategies in Tobacco necrosis virus-D. *Virology* 486, 54–62. doi: 10.1016/j.virol.2015.08.032
- Das, R., Laederach, A., Pearlman, S. M., Herschlag, D., and Altman, R. B. (2005). SAFA: semi-automated footprinting analysis software for high-throughput

FIGURE S3 | Importance of sequence complementarity for translation controlled by Ma5TE. *In vivo* cap-independent translation efficiency obtained in melon protoplasts of constructs with only the Ma5TE (45 nt) instead of the 3'-UTR flanking the 3'-end of the luciferase gene. A structure-stabilizing G-C clamp (+K) as described by Miras et al. (2017b) was added to the Ma5TE, as shown on the left. On the right: relative luciferase activity (%) shown as horizontal bars for each construct, as indicated. The activity of the wild-type construct 5'-end-luc-Ma5TE+K was set as 100%. Error bars represent the standard deviation of at least four independent experiments.

FIGURE S4 | Viral 5'-end secondary structure models. Schematic representation of the secondary structure prediction obtained with Mfold of the 5'-ends (between 180 and 240 nt) of the viral genomes **(A)** with I-shaped 3'-CITEs; **(B)** of the other carmoviruses apart from MNSV with proposed or identified 3'-CITEs; **(C)** of the tombusvirus CIRV. The arrows indicate the location of the identified complementary sequence stretches. Triangles denote the start of ORF1.

FIGURE S5 | Prediction of RNA interactions between the 5'-end and 3'-UTR of CarMV genomes. Bioinformatic prediction of possible functional interactions between the ends of MNSV genomes (Transat). Aligned sequences of all known CarMV genomes available in GenBank including the first 150 nt and the 3'-UTR sequence, separated by 10 adenines. Color of arched lines connecting interacting bases correspond to the estimated statistical significance of the interactions (*P*-value). Broken line arcs depict mutually exclusive helices. The maximal *P*-value threshold for the prediction was set at 0.03, the minimal stem length was 6. Highly conserved sequences appear in green in the alignment. The blue horizontal arrow marks the start codon of ORF1. Red vertical arrows mark the complementary nucleotides (amplified below) predicted to interact.

FIGURE S6 | Secondary structure prediction of the 5'-end of the MNSV genome. Prediction of the secondary structure using RNAalifold generated by structural alignment of the **(A)** 5'-UTRs and **(B)** 5'-ends (150 nt) of the MNSV genome sequences available in GenBank. Structure drawing with conservation annotation. Positions of nucleotide variations in the 5'-end sequences of other MNSV isolates that validate this model in double-stranded regions are marked with a circle; these variations do not disrupt base-pairing. Arrows indicate start codon (blue) and 3'-CITE interacting sequences (red).

TABLE S1 | Sequence stretches of the 5'-UTR or ORF1 with complementarity to I-shaped 3'-CITEs.

TABLE S2 | Sequence stretches localized in the 5'-UTR or ORF1 of carmovirus genomes with complementarity to their 3'-CITEs.

quantification of nucleic acid footprinting experiments. *RNA* 11, 344–354. doi: 10.1261/rna.7214405

- Díaz, J. A., Bernal, J. J., Moriones, E., and Aranda, M. A. (2003). Nucleotide sequence and infectious transcripts from a full-length cDNA clone of the carmovirus Melon necrotic spot virus. *Arch. Virol.* 148, 599–607. doi: 10.1007/s00705-002-0927-y
- Díaz, J. A., Nieto, C., Moriones, E., Truniger, V., and Aranda, M. A. (2004). Molecular characterization of a Melon necrotic spot virus strain that overcomes the resistance in melon and nonhost plants. *Mol. Plant Microbe Interact.* 17, 668–675. doi: 10.1094/MPMI.2004.17.6.668
- Díaz-Toledano, R., Lozano, G., and Martínez-Salas, E. (2017). In-cell SHAPE uncovers dynamic interactions between the untranslated regions of the foot-and-mouth disease virus RNA. *Nucleic Acids Res.* 45, 1416–1432. doi: 10.1093/nar/gkw795
- Fabian, M. R., and White, K. A. (2004). 5'-3' RNA-RNA interaction facilitates cap- and poly(A) tail-independent translation of Tomato bushy stunt virus mRNA: a potential common mechanism for tombusviridae. *J. Biol. Chem.* 279, 28862–28872. doi: 10.1074/jbc.M401272200
- Fabian, M. R., and White, K. A. (2006). Analysis of a 3'-translation enhancer in a tombusvirus: a dynamic model for RNA-RNA interactions of mRNA termini. *RNA* 12, 1304–1314. doi: 10.1261/rna.69506
- Fan, Q., Treder, K., and Miller, W. A. (2012). Untranslated regions of diverse plant viral RNAs vary greatly in translation enhancement efficiency. *BMC Biotechnol.* 12:22. doi: 10.1186/1472-6750-12-22

- Gao, F., Gulay, S. P., Kasprzak, W., Dinman, J. D., Shapiro, B. A., and Simon, A. E. (2013). The kissing-loop T-shaped structure translational enhancer of *Pea enation mosaic virus* can bind simultaneously to ribosomes and a 5' proximal hairpin. *J. Virol.* 87, 11987–12002. doi: 10.1128/jvi.02005-13
- Gao, F., Kasprzak, W., Stupina, V. A., Shapiro, B. A., and Simon, A. E. (2012). A ribosome-binding, 3' translational enhancer has a T-shaped structure and engages in a long-distance RNA-RNA interaction. *J. Virol.* 86, 9828–9842. doi: 10.1128/jvi.00677-12
- Gao, F., Kasprzak, W. K., Szarko, C., Shapiro, B. A., and Simon, A. E. (2014). The 3' untranslated region of *Pea enation mosaic virus* contains two T-shaped, ribosome-binding, cap-independent translation enhancers. *J. Virol.* 88, 11696–11712. doi: 10.1128/jvi.01433-14
- Gazo, B. M., Murphy, P., Gatchel, J. R., and Browning, K. S. (2004). A novel interaction of cap-binding protein complexes eukaryotic initiation factor (eIF) 4F and eIF(iso)4F with a region in the 3'-untranslated region of Satellite tobacco necrosis virus. *J. Biol. Chem.* 279, 13584–13592. doi: 10.1074/jbc.M311361200
- Guo, L., Allen, E., and Miller, W. A. (2000). Structure and function of a cap-independent translation element that functions in either the 3' or the 5' untranslated region. *RNA* 6, 1808–1820. doi: 10.1017/S1355838200001539
- Guo, L., Allen, E. M., and Miller, W. A. (2001). Base-pairing between untranslated regions facilitates translation of uncapped, nonpolyadenylated viral RNA. *Mol. Cell* 7, 1103–1109. doi: 10.1016/s1097-2765(01)00252-0
- Kierzek, R., Burkard, M. E., and Turner, D. H. (1999). Thermodynamics of single mismatches in RNA duplexes. *Biochemistry* 38, 14214–14223. doi: 10.1021/bi991186l
- Kneller, E. L. P., Rakotondrafara, A. M., and Miller, W. A. (2006). Cap-independent translation of plant viral RNAs. *Virus Res.* 119, 63–75. doi: 10.1016/j.virusres.2005.10.010
- Kraft, J. J., Treder, K., Peterson, M. S., and Miller, W. A. (2013). Cation-dependent folding of 3' cap-independent translation elements facilitates interaction of a 17-nucleotide conserved sequence with eIF4G. *Nucleic Acids Res.* 41, 3398–3413. doi: 10.1093/nar/gkt026
- Kuhlmann, M. M., Chattopadhyay, M., Stupina, V. A., Gao, F., and Simon, A. E. (2016). An RNA element that facilitates programmed ribosomal readthrough in Turnip crinkle virus adopts multiple conformations. *J. Virol.* 90, 8575–8591. doi: 10.1128/jvi.01129-16
- Liu, Z.-Y., Li, X.-F., Jiang, T., Deng, Y.-Q., Ye, Q., Zhao, H., et al. (2016). Viral RNA switch mediates the dynamic control of flavivirus replicase recruitment by genome cyclization. *eLife* 5:e17636. doi: 10.7554/eLife.17636
- Martin, F., Barends, S., Jaeger, S., Schaeffer, L., Prongidi-Fix, L., and Eriani, G. (2011). Cap-assisted internal initiation of translation of histone H4. *Mol. Cell* 41, 197–209. doi: 10.1016/j.molcel.2010.12.019
- Meulewaeter, F., Danthinne, X., Van Montagu, M., and Cornelissen, M. (1998a). 5'- and 3'-sequences of satellite tobacco necrosis virus RNA promoting translation in tobacco. *Plant J.* 14, 169–176. doi: 10.1046/j.1365-313X.1998.00104.x
- Meulewaeter, F., Van Montagu, M., and Cornelissen, M. (1998b). Features of the autonomous function of the translational enhancer domain of satellite tobacco necrosis virus. *RNA* 4, 1347–1356. doi: 10.1017/S135583829898092X
- Miller, W. A., and White, K. A. (2006). Long-distance RNA-RNA interactions in plant virus gene expression and replication. *Annu. Rev. Phytopathol.* 44, 447–467. doi: 10.1146/annurev.phyto.44.070505.143353
- Miras, M., Miller, W. A., Truniger, V., and Aranda, M. A. (2017a). Non-canonical translation in plant RNA viruses. *Front. Plant Sci.* 8:494. doi: 10.3389/fpls.2017.00494
- Miras, M., Sempere, R. N., Kraft, J. J., Miller, W. A., Aranda, M. A., and Truniger, V. (2014). Interfamilial recombination between viruses led to acquisition of a novel translation-enhancing RNA element that allows resistance breaking. *New Phytol.* 202, 233–246. doi: 10.1111/nph.12650
- Miras, M., Sempere, R. N., Kraft, J. J., Miller, W. A., Aranda, M. A., and Truniger, V. (2015). Determination of the secondary structure of an RNA fragment in solution: selective 2'-hydroxyl acylation analyzed by primer extension assay (SHAPE). *Bio Protoc.* 5:e1386. doi: 10.21769/BioProtoc.1386
- Miras, M., Truniger, V., Querol-Audi, J., and Aranda, M. A. (2017b). Analysis of the interacting partners eIF4F and 3'-CITE required for *Melon necrotic spot virus* cap-independent translation. *Mol. Plant Pathol.* 18, 635–648. doi: 10.1111/mpp.12422
- Mortimer, S. A., and Weeks, K. M. (2008). Time-resolved RNA SHAPE chemistry. *J. Am. Chem. Soc.* 130, 16178–16180. doi: 10.1021/ja8061216
- Nicholson, B. L., and White, K. A. (2008). Context-influenced cap-independent translation of Tombusvirus mRNAs in vitro. *Virology* 380, 203–212. doi: 10.1016/j.virol.2008.08.003
- Nicholson, B. L., and White, K. A. (2011). 3' Cap-independent translation enhancers of positive-strand RNA plant viruses. *Curr. Opin. Virol.* 1, 373–380. doi: 10.1016/j.coviro.2011.10.002
- Nicholson, B. L., Wu, B., Chevchenko, I., and White, K. A. (2010). Tombusvirus recruitment of host translational machinery via the 3' UTR. *RNA* 16, 1402–1419. doi: 10.1261/rna.2135210
- Nicholson, B. L., Zaslaver, O., Mayberry, L. K., Browning, K. S., and White, K. A. (2013). Tombusvirus Y-shaped translational enhancer forms a complex with eIF4F and can be functionally replaced by heterologous translational enhancers. *J. Virol.* 87, 1872–1883. doi: 10.1128/jvi.02711-12
- Nieto, C., Morales, M., Orjeda, G., Clepet, C., Monfort, A., Sturbois, B., et al. (2006). An eIF4E allele confers resistance to an uncapped and non-polyadenylated RNA virus in melon. *Plant J.* 48, 452–462. doi: 10.1111/j.1365-313X.2006.02885.x
- Parisien, M., and Major, F. (2008). The MC-Fold and MC-Sym pipeline infers RNA structure from sequence data. *Nature* 452, 51–55. doi: 10.1038/nature06684
- Rakotondrafara, A., Polacek, C., Harris, E., and Miller, W. (2006). Oscillating kissing stem-loop interactions mediate 5' scanning-dependent translation by a viral 3'-cap-independent translation element. *RNA* 12, 1893–1906. doi: 10.1261/rna.115606
- Roberts, R., Mayberry, L. K., Browning, K. S., and Rakotondrafara, A. M. (2017). The *Triticum mosaic virus* 5' leader binds to both eIF4G and eIFiso4G for translation. *PLoS One* 12:e0169602. doi: 10.1371/journal.pone.0169602
- Rodríguez-Hernández, A. M., Gosálvez, B., Sempere, R. N., Burgos, L., Aranda, M. A., and Truniger, V. (2012). Melon RNA interference (RNAi) lines silenced for Cm-eIF4E show broad virus resistance. *Mol. Plant Pathol.* 13, 755–763. doi: 10.1111/j.1364-3703.2012.00785.x
- Romero-López, C., and Berzal-Herranz, A. (2009). A long-range RNA-RNA interaction between the 5' and 3' ends of the HCV genome. *RNA* 15, 1740–1752. doi: 10.1261/rna.1680809
- Romero-López, C., and Berzal-Herranz, A. (2017). The 5BSL3.2 functional RNA domain connects distant regions in the Hepatitis C virus genome. *Front. Microbiol.* 8:2093. doi: 10.3389/fmicb.2017.02093
- Sakharov, P. A., and Agalarov, S. (2016). Free initiation factors eIF4A and eIF4B are dispensable for translation initiation on uncapped mRNAs. *Biochemistry* 81, 1198–1204. doi: 10.1134/S0006297916100175
- Sambrook, J., and Russell, D. W. (2001). *Molecular Cloning: A Laboratory Manual*, 3rd Edn. Cold Spring Harbor, NY: Cold Spring Harbor Laboratory Press.
- Sandoval-Jaime, C., and Gutiérrez-Escobedo, A. L. (2009). Cellular proteins mediate 5'-3' end contacts of Norwalk virus genomic RNA. *Virology* 387, 322–330. doi: 10.1016/j.virol.2009.02.041
- Sarawaneeyaruk, S., Iwakawa, H.-O., Mizumoto, H., Murakami, H., Kaido, M., Mise, K., et al. (2009). Host-dependent roles of the viral 5' untranslated region (UTR) in RNA stabilization and cap-independent translational enhancement mediated by the 3' UTR of Red clover necrotic mosaic virus RNA1. *Virology* 391, 107–118. doi: 10.1016/j.virol.2009.05.037
- Scheets, K., Jordan, R., White, K. A., and Hernández, C. (2015). *Pelarspovirus*, a proposed new genus in the family *Tombusviridae*. *Arch. Virol.* 160, 2385–2393. doi: 10.1007/s00705-015-2500-5
- Simon, A. E. (2015). 3'UTRs of carmoviruses. *Virus Res.* 206, 27–36. doi: 10.1016/j.virusres.2015.01.023
- Simon, A. E., and Miller, W. A. (2013). 3' cap-independent translation enhancers of plant viruses. *Annu. Rev. Microbiol.* 67, 21–42. doi: 10.1146/annurev-micro-092412-155609
- Stupina, V. A., Yuan, X., Meskauskas, A., Dinman, J. D., and Simon, A. E. (2011). Ribosome binding to a 5' translational enhancer is altered in the presence of the 3' untranslated region in cap-independent translation of *Turnip crinkle virus*. *J. Virol.* 85, 4638–4653. doi: 10.1128/jvi.00005-11
- Treder, K., Pettit Kneller, E. L., Allen, E. M., Wang, Z., Browning, K. S., and Miller, W. A. (2008). The 3' cap-independent translation element of Barley yellow dwarf virus binds eIF4F via the eIF4G subunit to initiate translation. *RNA* 14, 134–147. doi: 10.1261/rna.777308
- Truniger, V., Miras, M., and Aranda, M. A. (2017). Structural and functional diversity of plant virus 3'-cap-independent translation enhancers (3'-CITEs). *Front. Plant Sci.* 8:2047. doi: 10.3389/fpls.2017.02047

- Truniger, V., Nieto, C., Gonzalez-Ibeas, D., and Aranda, M. (2008). Mechanism of plant eIF4E-mediated resistance against a Carmovirus (*Tombusviridae*): cap-independent translation of a viral RNA controlled *in cis* by an (a)virulence determinant. *Plant J.* 56, 716–727. doi: 10.1111/j.1365-313X.2008.03630.x
- van Regenmortel, M. H. V., Fauquet, C. M., Bishop, D. H. L., Carstens, E. B., Estes, M. K., Lemon, S. M., et al. (2000). *Virus Taxonomy: Seventh Report of the International Committee on Taxonomy of Viruses*. San Diego, CA: Academic Press.
- Wang, Z., Kraft, J. J., Hui, A. Y., and Miller, W. A. (2010). Structural plasticity of Barley yellow dwarf virus-like cap-independent translation elements in four genera of plant viral RNAs. *Virology* 402, 177–186. doi: 10.1016/j.virol.2010.03.025
- Wang, Z., Parisien, M., Scheets, K., and Miller, W. A. (2011). The cap-binding translation initiation factor, eIF4E, binds a pseudoknot in a viral cap-independent translation element. *Structure* 19, 868–880. doi: 10.1016/j.str.2011.03.013
- Wang, Z., Treder, K., and Miller, W. A. (2009). Structure of a viral cap-independent translation element that functions via high affinity binding to the eIF4E subunit of eIF4F. *J. Biol. Chem.* 284, 14189–14202. doi: 10.1074/jbc.M808841200
- Wiebe, N. J. P., and Meyer, I. M. (2010). Transat—A method for detecting the conserved helices of functional RNA structures, including transient, pseudo-knotted and alternative structures. *PLoS Comput. Biol.* 6:e1000823. doi: 10.1371/journal.pcbi.1000823
- Zhang, J., Roberts, R., and Rakotondrafara, A. M. (2015). The role of the 5' untranslated regions of *Potyvirus* in translation. *Virus Res.* 206, 74–81. doi: 10.1016/j.virusres.2015.02.005
- Zhao, P., Liu, Q., Miller, W. A., and Goss, D. J. (2017). Eukaryotic translation initiation factor 4G (eIF4G) coordinates interactions with eIF4A, eIF4B, and eIF4E in binding and translation of the barley yellow dwarf virus 3' cap-independent translation element (BTE). *J. Biol. Chem.* 292, 5921–5931. doi: 10.1074/jbc.M116.764902

Conflict of Interest Statement: The authors declare that the research was conducted in the absence of any commercial or financial relationships that could be construed as a potential conflict of interest.

Copyright © 2018 Miras, Rodríguez-Hernández, Romero-López, Berzal-Herranz, Colchero, Aranda and Truniger. This is an open-access article distributed under the terms of the Creative Commons Attribution License (CC BY). The use, distribution or reproduction in other forums is permitted, provided the original author(s) and the copyright owner are credited and that the original publication in this journal is cited, in accordance with accepted academic practice. No use, distribution or reproduction is permitted which does not comply with these terms.